

Micromachined Linear Brownian Motor: Transportation of Nanobeads by Brownian Motion Using Three-Phase Dielectrophoretic Ratchet

Ersin ALTINTAS*, Karl F. BÖHRINGER¹, and Hiroyuki FUJITA

Center for International Research on Micro-Mechatronics, Institute of Industrial Science, The University of Tokyo, 4-6-1 Komaba, Meguro-ku, Tokyo 153-8505, Japan

¹Department of Electrical Engineering, The University of Washington, Box 352500,

234 Electrical Engineering/Computer Science Engineering Building, Seattle, WA 98195-2500, U.S.A.

(Received June 20, 2008; revised August 7, 2008; accepted August 15, 2008; published online November 14, 2008)

Nanosystems operating in liquid media may suffer from random Brownian motion due to thermal fluctuations. Biomolecular motors exploit these random fluctuations to generate a controllable directed movement. Inspired by nature, we proposed and realized a nano-system based on Brownian motion of nanobeads for linear transport in microfluidic channels. The channels limit the degree-of-freedom of the random motion of beads into one dimension, which was rectified by a three-phase dielectrophoretic ratchet biasing the spatial probability distribution of the nanobead towards the transportation direction. We micromachined the proposed device and experimentally traced the rectified motion of nanobeads and observed the shift in the bead distribution as a function of applied voltage. We identified three regions of operation: (1) a random motion region, (2) a Brownian motor region, and (3) a pure electric actuation region. Transportation in the Brownian motor region required less applied voltage compared to the pure electric transport. [DOI: [10.1143/JJAP.47.8673](https://doi.org/10.1143/JJAP.47.8673)]

KEYWORDS: Brownian motion, dielectrophoresis, flashing ratchet, nanobead, net-unidirectional motion, PDMS, transportation

1. Introduction

Brownian motion is random motion of microscopic particles in liquids due to thermal fluctuations. It is one of the dominating phenomena at the nanoscale.^{1,2} Feynman popularized it in his lectures to explain the possibility to rectify Brownian motion in order to obtain a directed motion by using a mechanical ratchet operated far from thermal equilibrium.³ Instead of the thermo-mechanical ratchet that was difficult to implement, the use of switching periodic asymmetrical potentials, so-called Brownian ratchets (motors), was proposed. Although most of the studies are concentrated on theoretical investigations^{4–6} and simulations,^{7,8} some practical implementations of the ratchets were reported as well in different areas such as particle pumping,⁹ separation and/or transport of particles^{10,11} or DNA.¹² The ratchets have provided a model for artificial molecular motors and machines.^{13,14} Furthermore, biophysicists are able to explain the working mechanism of bio-molecular motors, e.g., myosin.^{15–17} Bio-molecular motors exploit random thermal fluctuations to obtain a directed motion on predefined paths.^{6,17,18} Taking the above into consideration, Brownian motion is a good candidate of being a motive force for the actuation of nanoscale objects.

This work aims to develop a device called a linear Brownian motor (LBM), which exploits random thermal fluctuations to achieve the linear transport of nanoscopic particles in microchannels of comparable sizes as the particles. We employ micromachined electrodes to provide a multi-phase dielectrophoretic (DEP) rectification in order to bias the spatial probability distribution of the nanoparticles. This is different from the popular asymmetric (saw-tooth shape) and periodic potentials,^{4–6} where electrical force is directly responsible to move the particles to potential minima. In our device, the displacement between electrodes is achieved by Brownian motion of the particle itself. Consequently, the required voltage and energy

consumption are lower when thermal energy is utilized for the transportation of the particle as compared to a pure electric transportation.

2. Principle

Biomolecular motors move unidirectionally on some guiding structures such as microtubules in kinesin and actin filament in myosin.^{16–18} Those structures constrain the motion of biomolecular motors into one direction. This inspired us to tame the random motion and limit the degree-of-freedom of nanoparticles by using some microchannels. However, if even we achieve to tame the motion, it will be random motion in one dimension (1D). We propose to use a ratchet based on DEP force to direct the random motion.

The working principle of the Brownian motor is given in Fig. 1. A bead is initially trapped on an electrode (a–b) in a channel containing de-ionized water (DIW). By switching off the voltage, the bead starts Brownian motion and the probability density function of a bead position becomes wider (c). Then, the electrodes of the next phase are energized. The bead is able to move between electrically inactive electrodes. However, when the bead happens to come to the active electrode, it is trapped on that electrode and the density function will be like the one shown in (d). By continuing this flashing procedure, the probability of the transportation of the bead to the right will be higher than to the left. Since the applied voltage is lower than the one needed for a pure electrostatic transportation (direct attraction of a bead by active electrode from the adjacent inactive electrode), the thermal energy causing Brownian motion contributes for the transportation of the bead.

Our device (Fig. 2) employs microchannels to limit the three-dimensional (3D) random motion of nanobeads to 1D motion. Three-phase electrodes rectify this 1D motion. The equally spaced electrodes are 3 μm in width and separated from each other by 2 μm , which are reasonable dimensions for conventional lithography. Due to observation limitations, the diameter of the nanobead was selected as 0.5 μm . The depth and the widths of the channel were designed as 1 and

*E-mail address: ersin@iis.u-tokyo.ac.jp

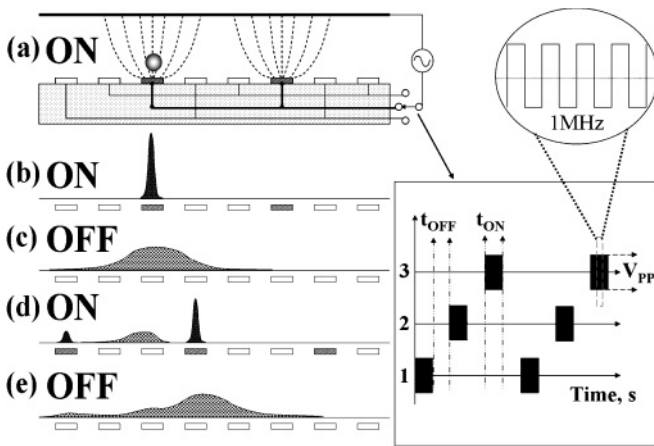


Fig. 1. Principle of a micromachined linear Brownian motor and three-phase dielectrophoretic ratchet. (a–b) Trapping of a bead on an active electrode. (c) Probability distribution of the bead position due to Brownian motion. (d) Activation of the next phase and trapping of the bead. On the inactive electrodes, diffusion continues since electrostatic force is not sufficient to attract a bead directly. (e) Next Brownian motion step. Repetitive ON/OFF cycling of three-phase produces net-unidirectional motion.

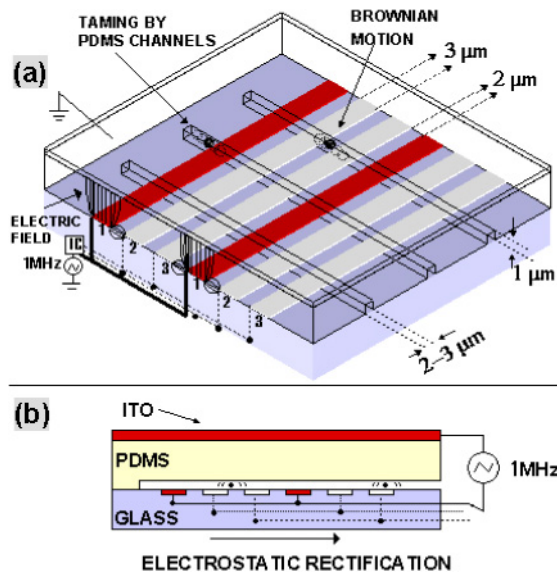


Fig. 2. (Color online) (a) Schematic of micromachined linear Brownian motor. Patterned PDMS sheet on a glass substrate provides microchannels. 3D Brownian motion is tamed in microchannel and turned into 1D motion. ITO line electrodes of $3\mu\text{m}$ wide and $2\mu\text{m}$ spacing were made on the glass substrate. The channels and the electrode were placed orthogonally to each other. Three-phase electrostatic field rectifies this random motion. (E-field is shown on the left side only. Device is not to scale.) (b) Cross-section of fabricated device. PDMS microchannel depth is $1\mu\text{m}$ and one end is closed.

$2\mu\text{m}$, respectively. 3D random motion of the nanobead is tamed in an easy, simple and inexpensive way.

During the rectification, the electrostatic trapping force is kept small enough to prevent attraction of the bead directly from the adjacent inactive electrodes, but sufficient to counteract the Brownian force on the active electrode. A bead travels from one electrode to the next by Brownian motion and so the energy used for the unidirectional transport is reduced. With the rectification in one direction, the probability that the bead moves in that direction becomes

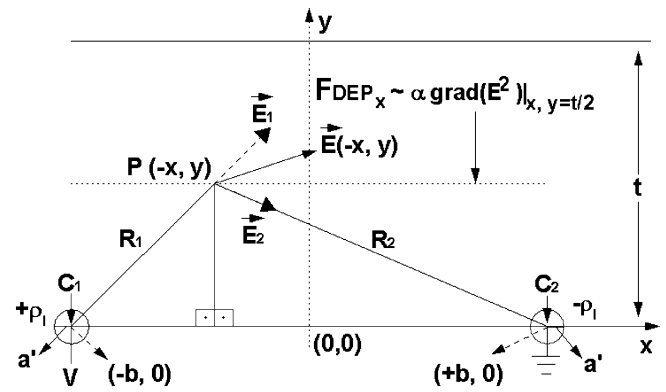


Fig. 3. Electrical field calculation by the image charge method. Line electrodes are represented by cylindrical conductors with a radius corresponding to the half of the thickness of fabricated electrodes. Center-to-center separation is $2b$. Potential difference between electrodes is V and charge density per unit length is ρ_l . The distances of the point $P(-x, y)$ to the imaginary charges are R_1 and R_2 , respectively. Gradient of electrical field squared with respect to x gives dielectrophoretic force in x direction keeping y as constant at the center of the channel.

higher than the probability that it moves in the opposite direction. These arguments imply an operation window for LBM. We utilize two phenomena in our motor; Brownian motion and electric force on a particle at high frequencies. This force causes dielectrophoresis (DEP), which is the induced motion of a polarizable particle in a non-uniform electrical field.^{19,20} Time averaged forced on a particle can be given by

$$\langle F_{\text{DEP}} \rangle = 2\pi a^3 \epsilon_m \text{Re}\{f_{\text{CM}}\} \nabla |E_{\text{rms}}|^2, \quad (1)$$

where a is the radius of the nanobead, ϵ_m is the permittivity of medium ($\epsilon_{\text{DIW}} = 80\epsilon_0$, where ϵ_0 is the permittivity of vacuum), $\text{Re}\{f_{\text{CM}}\}$ is the real part of the Clausius–Mossotti factor, which changes between 1 and -0.5 for a spherical particle, and E_{rms} is the root-mean-squared electrical field strength, respectively.^{19–21} The force is dependent on the gradient of electric field squared. The real part of the Clausius–Mossotti factor can be taken as 1, which is commonly done. In the simplest case, Brownian force can be estimated as follows. Let us assume that each segment of random motion is in the order of the diameter of the nanobead, $2a$. The particle has the same thermal energy, kT (k is Boltzmann’s constant and T is the absolute temperature of the medium, respectively), as the surrounding liquid molecules. This energy should be equal to the work done by Brownian force acting over $2a$. Therefore, Brownian force is estimated to be equal to $kT/2a$.²²

To estimate the necessary field strength and force that counteract the Brownian force (threshold force), we assume that a pair of active and inactive electrodes can be represented by two conducting cylinders of radius a' and of infinite length (Fig. 3). The field can be solved analytically by the image charge method.²³ Charges on electrodes can be replaced by two imaginary line charges located inside the cylindrical electrode. We can determine the charge density of line charges from the applied voltage between them. Exactly speaking, each line charge is not located at the center of the cylinder. This offset can be neglected if the diameter of cylinders is much smaller than their separation,

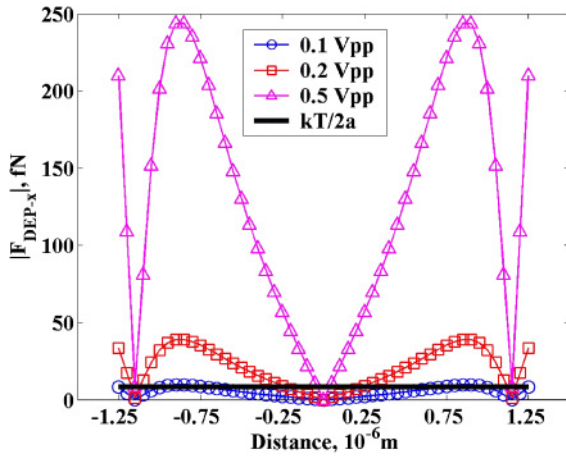


Fig. 4. (Color online) Dielectrophoretic (DEP) force at the center of channel by analytical calculation proposed in Fig. 3. Center-to-center distance of electrode, the depth of the channel, radius of the nanobead and the diameter of the electrodes are assumed as 2.5, 1, 0.25, and 0.05 μm , respectively. Force is calculated at room temperature in DIW. As compared to the threshold force, $kT/2a$, associated with Brownian motion, DEP force at 0.05 V_{rms} (0.1 V_{pp} , square wave) is small. At 0.25 V_{rms} (0.5 V_{pp} , square wave) and higher, DEP force dominates over threshold force.

which holds in our case. We will calculate the electrical field at a point, $P(-x, y)$, at the center of the channel ($y = t/2$, where t is the depth of the channel.). The distances between P and two line charges located at C_1 and C_2 are R_1 and R_2 , respectively. The electric field is given by the formula:

$$E_1 = \frac{\rho_l}{2\pi\epsilon_0 R_1} \frac{\vec{C}_1 P}{|C_1 P|} \quad \text{and} \quad E_2 = \frac{\rho_l}{2\pi\epsilon_0 R_2} \frac{\vec{P} C_2}{|P C_2|}. \quad (2)$$

We can find electric field, E , by vector addition as

$$E = E_1 + E_2. \quad (3)$$

By taking the gradient of the absolute value of E squared, we can calculate the DEP force in the longitudinal direction at the center of the channel analytically.

$$\nabla|E|^2 = \frac{\partial E^2}{\partial x} \Big|_{y=0.5 \mu\text{m}} \quad (4)$$

We have calculated the force for different applied voltages and the radius of the cylinders was set to 100 nm with a separation of 2.5 μm (Fig. 4). By comparing the DEP force to the threshold force, we can conclude that 0.05 V_{rms} (0.1 V_{pp} , square wave) is the lower limit to put a control on the bead. Increasing the voltage increases the force. At 0.25 V_{rms} and higher, the DEP force is much stronger than the threshold force. Above this region, particles will be attracted or transported electrostatically. Consequently, we experimentally operated the system between 0.1 V_{rms} (0.2 V_{pp}) and 0.5 V_{rms} (1 V_{pp}) at 1 MHz and examined the motion of particles to identify three regions of operation that are (1) a random motion region, (2) a Brownian motor region, and (3) a pure electric actuation region.

3. Experiments

3.1 Fabrication

Our experimental device consists of a cover glass (Matsunami, $24 \times 36 \text{mm}^2$) with indium tin oxide (ITO)

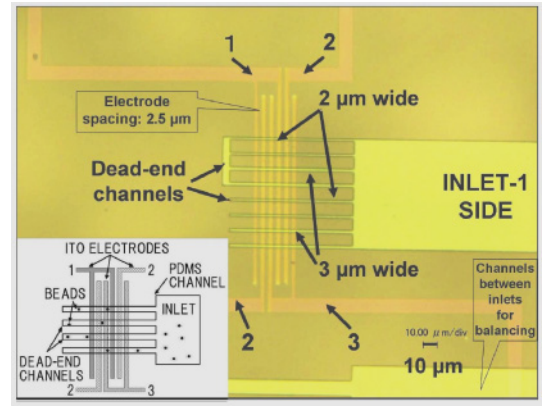


Fig. 5. (Color online) Digital microscope image of fabricated device (Keyence VHX-500). Two pairs of three-phase ITO electrodes are aligned with the dead-end PDMS microchannels. Electrode spacing is 2.5 μm . The width of the channels are 2 and 3 μm . Depth is 1 μm . Left-bottom is the schematic.

electrodes covered by a poly(dimethylsiloxane) (PDMS) sheet with microchannels aligned to the electrodes [Figs. 2(b) and 5]. For the electrode fabrication, we used a lift-off process. First, a S1818 photoresist (Shipley) of 2 μm thickness was patterned on the glass. After the postbake of the resist, the glass was isotropically etched in a buffered hydrofluoric acid (BHF, 1%) for 30 s to a depth of 100 nm in order to facilitate the lift-off process. After etching, a 100 nm thick ITO layer was sputter-deposited and a lift-off process was performed by dissolving the photoresist with acetone in an ultrasonic bath. PDMS microchannels were prepared from a silicon (Si) mold. Si substrate was cleaned first and then spin-coated by the same photoresist. After patterning, Si was etched in deep reactive ion etching (STS MultiPlex ASE, ST3644) system for 1 μm with a process used for photonic crystals. After removal of the photoresist, the surface of the substrate was modified by CHF_3 plasma in a reactive ion etching system (Samco RIE-10NR) to enhance the removal of PDMS from the mold.^{24,25} The mixture for PDMS was prepared from silicone elastomer, curing agent and FZ-77, respectively (500 : 50 : 1 by weight, Dow Corning). PDMS is hydrophobic,²⁶ hence we included FZ-77 to make it hydrophilic to fill the bead suspension by capillary forces in the microchannel. After mixing, it was degassed, and poured onto the Si mold, and spin coated (300 rpm–60 s, 3000 rpm–2 s). Following this, PDMS was cured at 110 $^\circ\text{C}$ on a hot plate for 1 h. The thickness around the channels was measured as $93 \pm 2 \mu\text{m}$. The PDMS sheet was peeled off and inlets were punched and opened. The channels were optically aligned by an aligner (Union PEM-4) with ITO electrodes.

3.2 Procedure

Experimental observations were performed with an inverted microscope (Olympus IX71). The aligned sample was fixed onto a pinch board whose center had a hole for the objective of the microscope. The sample was fixed onto the stage of the microscope and electrical connections were provided by a conductive tape. An IC circuitry switched ratcheting voltage. Light-emitting-diodes were used at the outputs of the circuit to synchronize the system with the recording apparatus (Sony RDR-HX10). Diluted suspen-

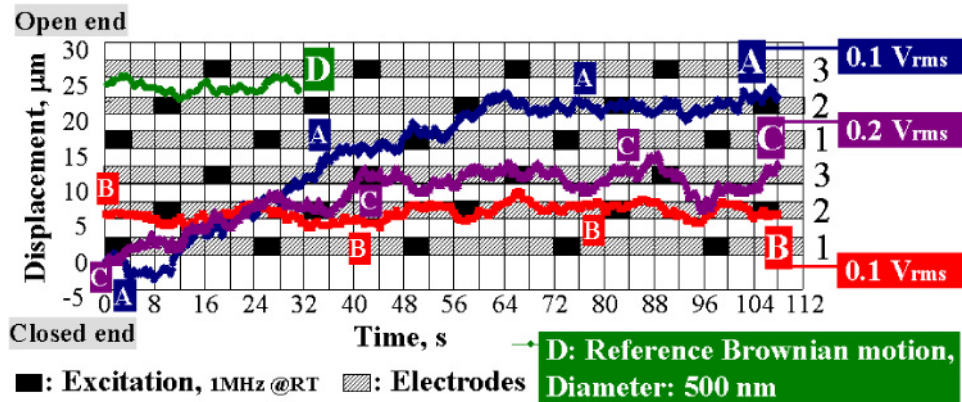


Fig. 6. (Color online) Rectified Brownian motion of nanobeads and net-unidirectional motion to the open end. Nanobead A is transported over $20\mu\text{m}$ in 100 s, while nanobead B wanders around. This eliminates the possibility of a bias due to micro-flows or electrostatic attraction. Inverse motion is possible in Brownian motor due to random nature of the motion. Trapping mainly occurs at the electrode corners due to dielectrophoretic effects. Square wave at 0.1 and $0.2 V_{\text{rms}}$ -1MHz is applied. Electrodes are superimposed to the displacement graph. Black rectangles stand for excitation of the electrode and correspond to 4 s. Time-scale errors are around 0.2 s. Due to fabrication, electrode separation is $2.5\mu\text{m}$ rather than $2\mu\text{m}$.

sion of fluorescent nanobeads [fluoresbrite plain microspheres, 2.5% solid latex, $0.5\mu\text{m}$, yellow-green, Polysciences, 1 (initial concentration) : 800 (DIW)] was injected into the inlet. After it reached the microchannels, the second injection was done from the second inlet, and then it was left untouched until stabilization was achieved. During the injection, it was observed that air leaked out either through inlets and/or PDMS, which was gas permeable.^{26,27} The counter ITO electrode consisting of the coverglass whose both sides had sputter-coated by ITO was placed on the PDMS sheet. 1D random motion of the beads was confirmed by the optical microscope.

The system was operated and recorded with a speed of 30 frames/s. The recorded video in AVI format was analyzed by the tracking analysis software, Cosmos. The excitation of the electrodes or rectification was performed from the closed end to the open end to eliminate any bias related to the micro/nano flows that could be caused by inlets. A nanobead with a diameter of 500nm in DIW at room temperature has a diffusion constant of $0.987\mu\text{m}^2/\text{s}$ and a root-mean-square displacement of $2.8\mu\text{m}$ in 4 s in DIW at room temperature. This time interval is sufficient for the nanobeads to experience Brownian motion and to diffuse easily between electrodes with $2\mu\text{m}$ (or $2.5\mu\text{m}$) of spacing. We applied voltage at the high frequency because an undesirable liquid flow was created at low frequencies due to AC electro-osmosis (fluid motion caused by interaction of ions in the double layer with electrical field).^{19,20} We applied the voltages between 0.1 to $0.5 V_{\text{rms}}$. Electrodes of one phase were switched on and off for 4 s successively and shown as horizontal bars in the displacement characteristic to simplify the visualization of the motion of the beads on or near to the electrodes.

4. Results and Discussion

The displacements of nanobeads, A ($0.1 V_{\text{rms}}$), B ($0.1 V_{\text{rms}}$), C ($0.2 V_{\text{rms}}$), and D (Brownian motion as a reference without voltage application), with time are given in Fig. 6. (Electrode spacing was $2.5\mu\text{m}$, which was believed to be caused by excessive etching of photomask in Cr etchant.) The nanobeads, A and C, move to the rectification direction

with occasional reverse motions. The graph indicates that nanobead A and C are transported over 20 and $10\mu\text{m}$, respectively, approximately in 100 s. While the motions of the bead A and, to some extent, the bead C are rectified with some backward motion, B wanders around. This shows the stochastic nature of LBM. Furthermore, this supports that the motion of A is not a linear motion due to electrostatic forces but a dielectrophoretically rectified Brownian motion in predefined direction. With the applied voltage between 0.1 and $0.2 V_{\text{rms}}$, the electrostatic field is only effective in the vicinity of the electrodes. This suggests those operation conditions correspond to the Brownian motor region.

We have worked with larger numbers of particles to investigate the net-displacements of the nanobeads at different voltage levels. Displacement videos are divided into 100 s, and the distance from final position to the initial position of the beads (net-displacements) are determined (Fig. 7). The mean value and standard deviation were calculated for each distribution. The distributions shift to the rectification direction with increasing voltage. According to experimental results, the random motion region is less than or around $0.1 V_{\text{rms}}$, where transportation is barely observed, even though we sometimes achieved the rectification (nanobead A, Fig. 6). (A finite resistance has been measured in ITO electrodes which may cause a voltage drop in the double layer and effective voltage might be slightly smaller than $0.1 V_{\text{rms}}$.¹⁹) Beads moved more obviously to one direction around $0.25 V_{\text{rms}}$, which we believe lies in the Brownian motor region or at the beginning of the pure electric actuation region. The shift is clear around $0.5 V_{\text{rms}}$. The tracking analyses around $0.5 V_{\text{rms}}$ showed abrupt displacements of the beads; this observation reinforces the existence of the directed motion due to external force. This suggests that it is in the electric actuation region.

Although we assume that Brownian motion and DEP forces are effective in the system, there can be different phenomena causing the motion of the beads. Those are mainly gravitational force with buoyancy, AC electro-osmosis, thermal flows, convection and electromagnetic forces. Our system operates at high frequency, 1 MHz, and uses 800 times diluted suspension of 500nm fluorescent nanobeads in DIW. Under

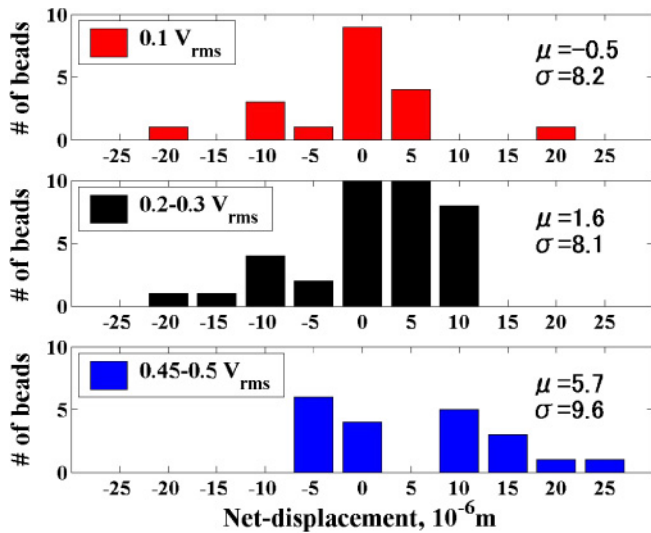


Fig. 7. (Color online) Displacement of nanobeads in 100 s at different excitation voltages. Increasing applied voltages shift the distribution to the rectification direction, i.e. to the right. Displacements are rounded to the nearest integer multiples of 5. μ and σ stand for the mean and the standard deviation of the distributions. Three particles at 0.5 V_{rms} displaced 10, 15, and 25 μm , respectively in 80 s.

these conditions, we carefully calculated those forces and came to the conclusion that the magnitudes of these phenomena are negligible compared to Brownian motion and DEP.^{19,20} Therefore, Brownian motion and dielectrophoretic rectification were dominant in our system.

In contrast to Brownian motors based on the asymmetric and periodic potentials,⁴⁻⁶ our system generates directed motion by utilizing a three-phase dielectrophoretic ratchet. Both approaches utilize an ON/OFF mechanism to take the system out of equilibrium. However, in case of asymmetrical potentials, during ON state, particle stays at or moves to potential minima, while in our case the particles are able to experience random motion. In asymmetrical potentials, the particle experiences Brownian motion during the OFF state. When the particle is trapped by the adjacent asymmetrical potential in the ON state, it is attracted to the potential minima by electrical forces.⁶⁾

In our system, in the Brownian motor region, we have achieved transportation of the nanobeads with lower applied voltages than the pure electric actuation region, which reduces energy consumption. However, smaller average values of distributions at lower voltages in a fixed time indicate an expected trade-off between energy saving and the average speed. As a result, our system is less effective in terms of positive transport of particles in a fixed time but reduces energy consumption.

The system can be further characterized by investigating different parameters which have some effect on Brownian motion and DEP force. These parameters include the switching time (ON and OFF time), dimensions (the particle size and the electrode spacing), and the medium (viscosity, temperature, and permittivity). We have been working on the experimental characterization of the net-transport of the beads by changing different parameters experimentally. We are also performing simulations to compare results with experiments and to determine the optimum region of operation.

5. Conclusions

We used a micromachined three-phase dielectrophoretic ratchet to rectify the Brownian motion of nanobeads in a linear microfluidic channel. By increasing the rectification voltage, we observed the transition from random motion to pure electric actuation of nanobeads. In the middle of those, there was a voltage window where the Brownian motion contributed to the transport of nanobeads in the predetermined direction. This study may lead to a better understanding of effective and efficient transportation of nanoparticles in artificial systems that exploit random thermal motion. To further strengthen the case for using random thermal motion as a driving mechanism, we are currently collecting statistical data on the transportation of larger numbers of particles by experimentally characterizing LBM with different parameters. These results will be compared with our models and simulations.

Acknowledgements

We would like to thank the Ministry of Education, Culture, Sports, Science and Technology, Japan, for financial support.

- 1) G. Oster: *Nature* **417** (2002) 25.
- 2) R. D. Astumian: *Sci. Am.* **285** (2001) 56.
- 3) R. P. Feynman, R. B. Leighton, and M. Sands: *The Feynman Lectures on Physics* (Addison-Wesley, Reading, MA, 1963) p. 46.1.
- 4) P. Hänggi, F. Marchesoni, and F. Nori: *Ann. Phys. (Leipzig)* **14** (2005) 51.
- 5) J. M. R. Parrondo and B. J. De Cisneros: *Appl. Phys. A* **75** (2002) 179.
- 6) H. Linke, M. T. Downton, and M. J. Zuckermann: *Chaos* **15** (2005) 026111.
- 7) A. Allison and D. Abbott: *Microelectron. J.* **33** (2002) 235.
- 8) M. P. Hughes: *J. Phys. D* **37** (2004) 1275.
- 9) S. Matthias and F. Müller: *Nature* **424** (2003) 53.
- 10) J. Rousselet, L. Salome, A. Ajdari, and J. Prost: *Nature* **370** (1994) 446.
- 11) E. Kamholz: *Nat. Mater.* **2** (2003) 507.
- 12) J. S. Bader, R. W. Hammond, S. A. Henck, M. W. Deem, G. A. McDermott, J. M. Bustillo, J. W. Simpson, G. T. Mulhern, and J. M. Rothberg: *Proc. Natl. Acad. Sci. U.S.A.* **96** (1999) 13165.
- 13) T. R. Kelly, H. D. Silva, and R. D. Silva: *Nature* **401** (1999) 150.
- 14) W. R. Browne and B. L. Feringa: *Nat. Nanotechnol.* **1** (2006) 25.
- 15) M. Bier: *Contemp. Phys.* **38** (1997) 371.
- 16) R. Ait-Haddou and W. Herzog: *Cell Biochem. Biophys.* **38** (2003) 191.
- 17) M. Schliwa: *Molecular Motors* (Wiley-VCH, Weinheim, 2003).
- 18) T. Yanagida, M. Ueda, T. Murata, S. Esaki, and Y. Ishii: *Biosystems* **88** (2007) 228.
- 19) A. Castellanos, A. Ramos, A. Gonzales, N. G. Green, and H. Morgan: *J. Phys. D* **36** (2003) 2584.
- 20) H. Morgan and N. G. Green: *AC Electrokinetics: Colloids and Nanoparticles* (RSP, Hertfordshire, U.K., 2003) p. 139.
- 21) M. Washizu, S. Suzuki, O. Kurosawa, T. Nishizaka, and T. Shinohara: *IEEE Trans. Ind. Appl.* **30** (1994) 835.
- 22) *Encyclopedia of Nanoscience and Nanotechnology*, ed. H. S. Nalwa (American Scientific Publishers, Valencia, CA, 2004) p. 623.
- 23) L. Solymar: *Lectures on Electromagnetic Theory* (Oxford University Press, Oxford, U.K., 1976) p. 33.
- 24) G. S. Oehrlein, Y. Zhang, D. Vender, and M. Haverlag: *J. Vac. Sci. Technol. A* **12** (1994) 323.
- 25) H. F. Arata, Y. Rondelez, H. Noji, and H. Fujita: *Anal. Chem.* **77** (2005) 4810.
- 26) H. Makamba, J. H. Jim, K. Lim, N. Park, and J. H. Hahn: *Electrophoresis* **24** (2003) 3607.
- 27) E. Verneuil, A. Buguin, and P. Silberzan: *Europhys. Lett.* **68** (2004) 412.